Journal of Electroceramics, 8, 195–202, 2002

Co-Modification of $Ba_5NdTi_3Ta_7O_{30}$ Dielectric Ceramics by Substitution and Introducing Secondary Phase

X.H. ZHENG & X.M. CHEN

Department of Materials Sciences & Engineering, Zhejiang University, Hangzhou 310027, People's Republic of China

Submitted June 25, 2001; Revised March 12, 2002; Accepted March 21, 2002

Abstract. Co-modification of $Ba_5NdTi_3Ta_7O_{30}$ dielectrics ceramics was investigated through Pb substitution for Ba and introducing $Bi_4Ti_3O_{12}$ secondary phase. The dielectric constant increased from 150 to 283, the temperature coefficient of the dielectric constant decreased from -2500 ppm/°C to -1279 ppm/°C, and the dielectric loss decreased to 0.0007 at 1 MHz. Meanwhile, the bi-phase ceramics were investigated to achieve temperature stable ceramics with high dielectric constant and low dielectric loss. As the composition x varied from 0.4 to 0.7 for $(1-x)(Ba_{0.8}Pb_{0.2})_5NdTi_3Ta_7O_{30}/xBi_4Ti_3O_{12}$, the temperature coefficient of the dielectric constant changed from negative to zero to positive.

Keywords: tungsten-bronze, $Ba_5NdTi_3Ta_7O_{30}$, $Bi_4Ti_3O_{12}$, dielectric properties

1. Introduction

New ferroelectric compounds in tungsten-bronze families, such as barium sodium niobate (BKN) [1], potassium lanthanum niobate (KLN) [2], barium strontium niobate (BSN) [3] have attracted much scientific and commercial interest because of their wide potential application. The tungsten-bronze compounds consist of a complex array of sharing corner distorted BO_6 octahedra in such a way that three different types of interstices (A, B and C) are available for cation substitutions in the general formula $(A_2)_4(A_1)_2(C)_4(B_1)_2(B_2)_8O_{30}$ [4]. It has been found that their physical properties can be improved by a large variety of ionic substitutions at the above-mentioned sites.

Recently, Chen et al. have proposed some promising candidates for high dielectric constant ($\varepsilon > 100$) dielectric ceramics with tungsten-bronze structure in the BaO-Nd_2O_3-TiO_2-Ta_2O_5 quaternary system [5, 6]. In the system, $Ba_4Nd_2Ti_4Ta_6O_{30}$ ceramics has been modified through Bi, Sr and Ti substitutions for Nd, Ba and Ta respectively, and the $Ba_4Nd_2Ti_4Ta_6O_{30}/(La_{0.9}Bi_{0.1})_2Ti_2O_7$ bi-phase system has also been investigated [7–10]. The temperature coefficient of the dielectric constant has been suppressed effectively by such ways. However, $Ba_5NdTi_3Ta_7O_{30}$ with higher dielectric constant and lower dielectric loss has not received enough attention due to its relatively larger temperature coefficient of the dielectric constant ($\tau_\varepsilon = -2500$ ppm/°C at 10 kHz) [5]. Meanwhile, it was reported that the layer structure compound $Bi_4Ti_3O_{12}$ has a high dielectric constant of 180, and a large positive temperature coefficient of the dielectric constant: 650 ppm/°C [11].

The capacitive volumetric efficiency can be increased and the corresponding dimensionality of a dielectric component can be significantly decreased through incorporating a high dielectric constant material. Temperature stability of the dielectric properties is a necessary requirement for many consumer applications such as mobile communications, automotive components, and portable electric devices [12].

Usually, PbO, Bi_2O_3 or $Bi_4Ti_3O_{12}$ is added to improve temperature stability and to decrease sintering temperature. Kolar et al. [13] reported that small additions of Bi_2O_3 or $Bi_4Ti_3O_{12}$ could improve the dielectric properties of $BaNd_2Ti_5O_{14}$ and $BaNd_2Ti_4O_{12}$ ceramics. Wu et al. [14] and Zheng et al. [15] reported $Bi_4Ti_3O_{12}$ modified $Ba_{6-3x}Nd_{8+2x}Ti_{18}O_{54}$ and $Ba_5NdTi_3Ta_7O_{30}$ ceramics, respectively.

In the present work, $Ba_5NdTi_3Ta_7O_{30}$ ceramics have been modified through Pb substitution for Ba and the (Ba, Pb)$_5NdTi_3Ta_7O_{30}/Bi_4Ti_3O_{12}$ bi-phase system is examined.

2. Experiments

All the samples were synthesized by conventional solid-state reaction methods from high-purity powders of $BaCO_3$(>99.93%), PbO(>99%), Bi_2O_3-(>99%), Nd_2O_3(>99%), TiO_2(>99.8%) and Ta_2O_5-(>99.99%). The raw powders were weighed according to the batch formula $(Ba_{1-x}Pb_x)_5NdTi_3Ta_7O_{30}$, $(1-x)(Ba_{0.8}Pb_{0.2})_5NdTi_3Ta_7O_{30}/xBi_4Ti_3O_{12}$, and ground in ethanol with ZrO_2 balls for 24 h. Then the powder mixtures were dried and calcined at 1100°C for $(Ba_{1-x}Pb_x)_5NdTi_3Ta_7O_{30}$ in air for 3 h, and the mixed powders of $(1-x)(Ba_{0.8}Pb_{0.2})$-$_5NdTi_3Ta_7O_{30}/xBi_4Ti_3O_{12}$ were calcined at 800°C for one hour first in order to prevent PbO and Bi_2O_3 volatilizing, then elevated to 1000°C for 3 hours. The powders were then reground for one day and dried, then mixed with organic binder of 5 wt% polyvinyl alcohol (PVA). The powders were pressed into pellets with a cylindrical shape of 12 mm in diameter and 2 to 4 mm in thickness at a pressure of 98 MPa. The disks of $(Ba_{1-x}Pb_x)_5NdTi_3Ta_7O_{30}$ were sintered in the temperature range from 1350°C to 1450°C in air for 3 h, and the disks of $(1-x)(Ba_{0.8}Pb_{0.2})$-$_5NdTi_3Ta_7O_{30}/xBi_4Ti_3O_{12}$ were sintered in the temperature range of 1100°C to 1200°C for 2 h.

The bulk density of the sintered samples was measured by the dimensional method. The microstructures were characterized by X-ray diffraction (XRD) using Cu K_α radiation and scanning electron microscopy (SEM). The dielectric properties at room temperature were characterized by an LCR meter (HP4285A) from 100 KHz to 10 MHz. The temperature coefficient of the dielectric constant was measured at 1 MHz by another LCR meter (HP4284A) equipped with a thermostat in the temperature range from room temperature to 85°C.

3. Results and Discussions

3.1. Pb Substitution for Ba

Compared with the end-member of $Ba_5NdTi_3Ta_7O_{30}$, the densification temperature of $(Ba_{1-x}Pb_x)_5NdTi_3$-Ta_7O_{30} ceramics decreased. The sintering characteristics of $(Ba_{1-x}Pb_x)_5NdTi_3Ta_7O_{30}$ ceramics are shown in Fig. 1. The disks cracked during sintering when x was more than 0.5. This is probably because of the change of structure. This is confirmed by SEM observation. As shown in Fig. 2, the grain morphology of $(Ba_{0.4}Pb_{0.6})$-$_5NdTi_3Ta_7O_{30}$ ceramics is different from that of the end-members. With increasing Pb content, the grain shape became plate-like, but there was only one kind of grain observed.

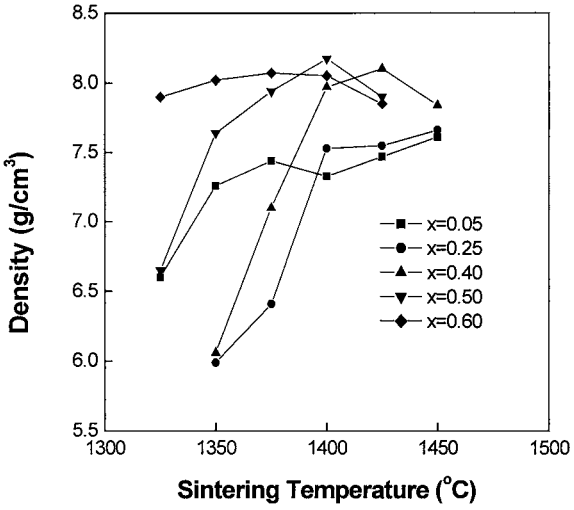

Fig. 1. Densities of $(Ba_{1-x}Pb_x)_5NdTi_3Ta_7O_{30}$ ceramics with various sintering temperatures for 3 h.

The peaks and intensities of XRD patterns of all the present ceramics are both corresponding to the $Ba_5NdTi_3Ta_7O_{30}$ phase. This agrees with the results of SEM observation. The crystal parameters are calculated from XRD data of the main peaks and refined with the least-squares method, and the results are shown in Table 1 and Fig. 3. When x is 0.05, the a, b axes become shorter, and the c axis does not change. Then the

Table 1. Variation of crystal parameters and theoretical densities of $(Ba_{1-x}Pb_x)_5NdTi_3Ta_7O_{30}$ ceramics.

X	0^{11}	0.05	0.25	0.40	0.5	0.6
$a(10^{-10}$ m)	12.4826	12.4424	12.4497	12.4640	12.4596	12.4406
$b(10^{-10}$ m)	12.4826	12.4424	12.4497	12.4640	12.4596	12.4406
$c(10^{-10}$ m)	3.9295	3.9295	3.9128	3.9140	3.9116	3.9330
$10^{1/2}c/a$	0.9955	0.9987	0.9939	0.9930	0.9928	0.9997
($\rho_t{}^a$) (g/cm^3)	7.38	7.48	7.69	7.81	7.92	8.00

[a] ρ_t is the theoretical density.

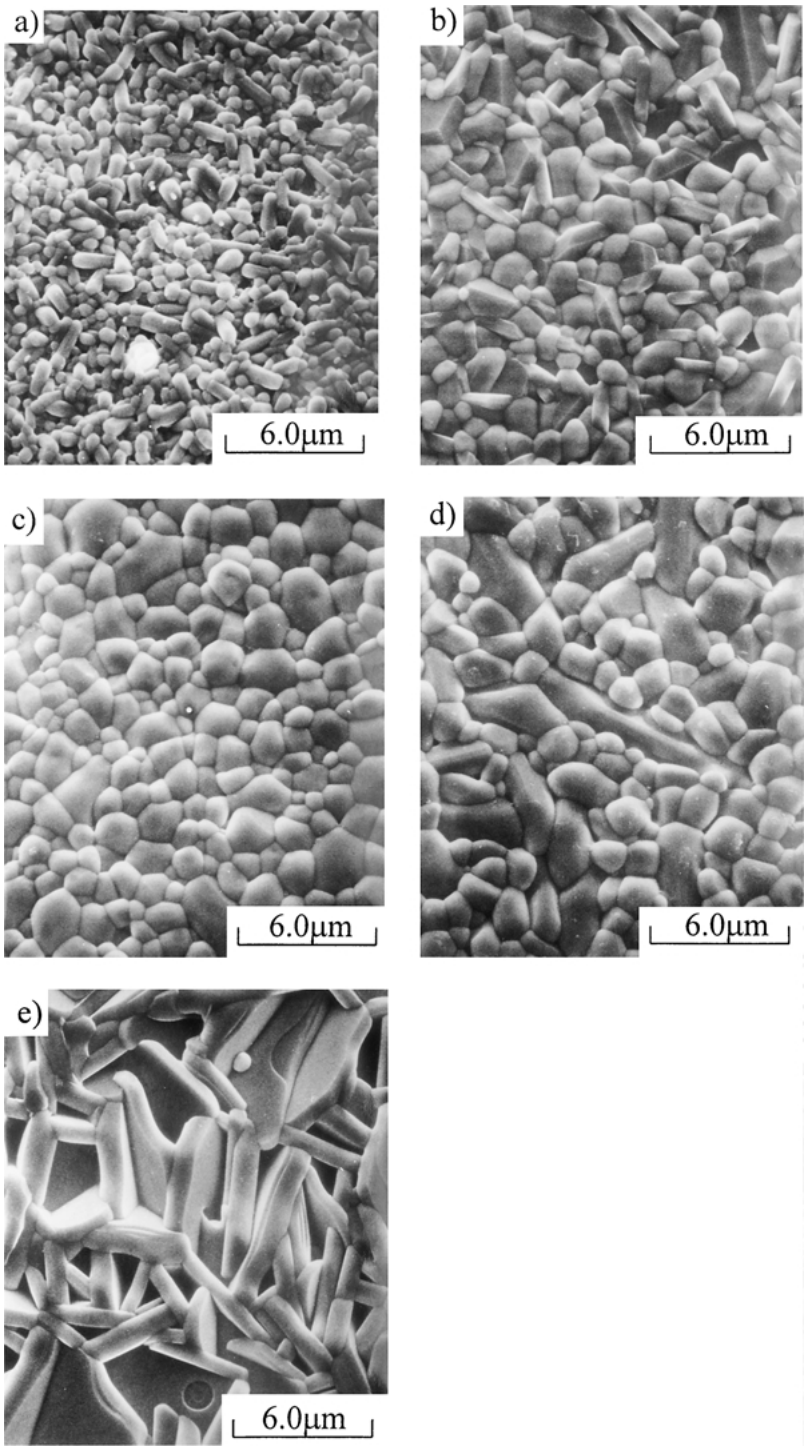

Fig. 2. SEM micrographs of $(Ba_{1-x}Pb_x)_5NdTi_3Ta_7O_{30}$ ceramics sintered at 1400°C in air for 3 h (a) $x = 0.05$, (b) $x = 0.25$, (c) $x = 0.40$, (d) $x = 0.50$, (e) $x = 0.60$ (sintered at 1375°C).

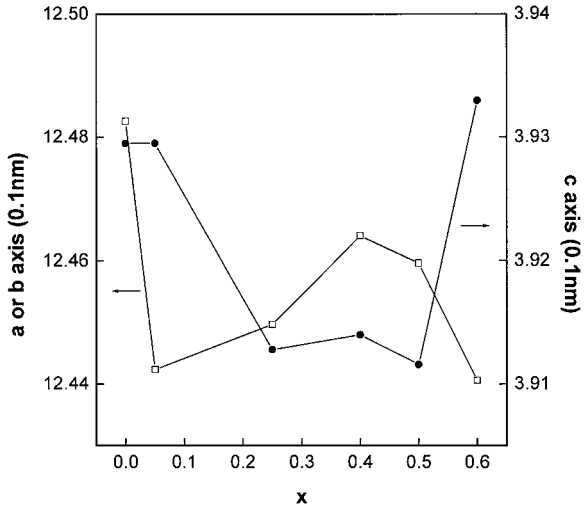

Fig. 3. Variation of the unit cell parameters of $(Ba_{1-x}Pb_x)_5NdTi_3Ta_7O_{30}$ dense ceramics.

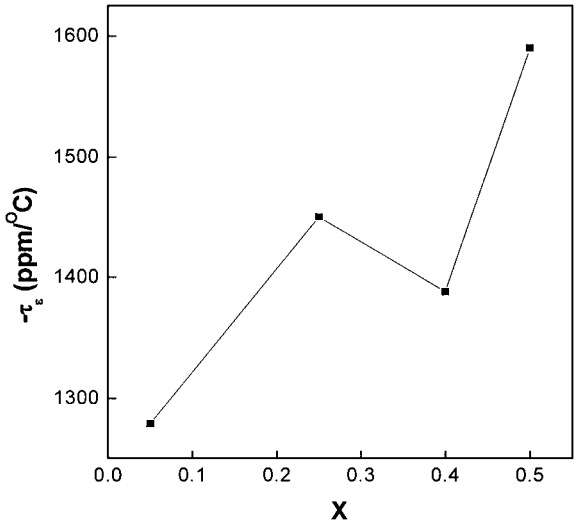

Fig. 5. Temperature coefficient of dielectric constant of $(Ba_{1-x}Pb_x)_5NdTi_3Ta_7O_{30}$ ceramics sintered at 1400°C for 3 h.

a, b axes increase slightly until $x = 0.4$, then decrease slightly. But the c axis becomes shorter when x is more than 0.05, however, the c axis increase rapidly as x is more than 0.5. This change of unit cell parameters is due to the smaller Pb^{2+} ions substitution for the larger Ba^{2+} ions and Pb volatilization during sintering.

The dielectric properties of dense $(Ba_{1-x}Pb_x)_5NdTi_3Ta_7O_{30}$ ceramics are shown in Figs. 4 and 5. The dielectric constant increases with increasing Pb content. This would be explained by Clausius-Mossotii

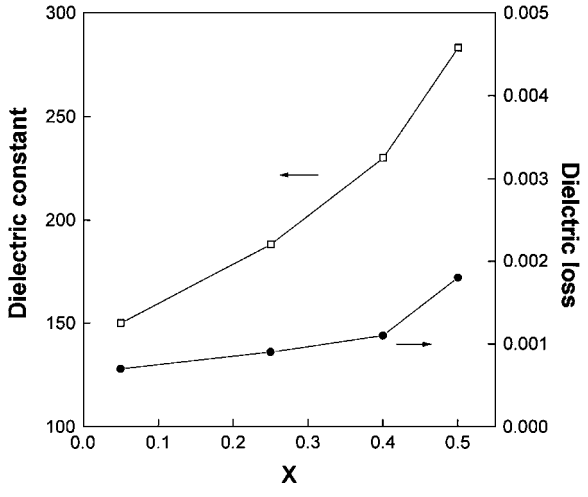

Fig. 4. Dielectric constant and dielectric loss of $(Ba_{1-x}Pb_x)_5NdTi_3Ta_7O_{30}$ ceramics sintered at 1400°C for 3 h.

formula [16]:

$$\varepsilon = \frac{3V + 8\pi\alpha_m}{3V - 4\pi\alpha_m} \tag{1}$$

where V is the volume of unit cell, α_m is the polarity of the unit cell. The smaller $Pb^{2+}(1.49 \times 10^{-10}\,m)$ ions substitution for the larger $Ba^{2+}(1.61 \times 10^{-10}\,m)$ ions [17] results in the decrease of unit cell volume, as shown in Table 1, and the polarizability $Ba^{2+}(6.40\times10^{-30}\,m^3)$ is smaller than that of $Pb^{2+}(6.58 \times 10^{-30}\,m^3)$ [18], so the dielectric constant increases with increasing Pb content. Meanwhile, the significant polarization contribution can be attributed to cations (Pb^{2+} and Ba^{2+}) at the A_2-sites. It is known that for lead-free oxygen octahedral compounds, the displacement of cations at the B-site from the oxygen plane is the major contribution to the macroscopic polarization. However, substantial polarization contribution can be attributed to the displacements of Pb^{2+} and Ba^{2+} ions at the A_2-sites, as they are of similar magnitude as that of the cations at the B-site. Therefore, the dielectric constant increases rapidly with Pb substitution for Ba.

The temperature coefficient of the dielectric constant was improved as expected. The change can be explained by the AKJ equation [19]:

$$T_C = k\Delta z_i^2 \tag{2}$$

where T_C is the Curie temperature, k is a constant and Δz_i is the atomic displacement. According to the AKJ equation, the Curie temperature of $(Ba_{1-x}Pb_x)_5NdTi_3Ta_7O_{30}$ shifts to lower temperature with atomic displacement Δz_i at the B-sites turns small because smaller Pb^{2+} ions substitute for larger Ba^{2+} ions. However, the atomic displacement Δz_i at the A_2-site becomes larger, which makes the Curie temperature higher. So the temperature coefficient of the present ceramics changes with the combination effects. Moreover, the Curie temperature of $Ba_5NdTi_3Ta_7O_{30}$ ceramics is below room temperature. So the temperature coefficient of the dielectric constant of $(Ba_{1-x}Pb_x)_5NdTi_3Ta_7O_{30}$ ceramics is improved when small content of Pb substitutes for Ba. τ_ε is improved significantly from -2500 ppm/°C to -1279 ppm/°C at $x = 0.05$. Meanwhile, the dielectric loss of the present ceramics was on the order of 10^{-4}.

3.2. *(1−x) $(Ba_{0.8}Pb_{0.2})NdTi_3Ta_7O_{30}/xBi_4Ti_3O_{12}$ System*

The XRD patterns in Fig. 6 point to a two phases structure in all compositions, i.e. $Ba_5NdTi_3Ta_7O_{30}$ and $Bi_4Ti_3O_{12}$ phases. However, some weak peaks of $Pb_2Ti_2O_6$ phase are presented for the composition $x = 0.5$. With increasing $Bi_4Ti_3O_{12}$ content, the major phase varies from the $Ba_5NdTi_3Ta_7O_{30}$ phase to the $Bi_4Ti_3O_{12}$ phase. Regardless, the content of the $Pb_2Ti_2O_6$ phase, and the contents of $Ba_5NdTi_3Ta_7O_{30}$ and $Bi_4Ti_3O_{12}$ were calculated by the following equations:

$$W_T = \frac{I_{max}(\text{Tungsten})}{I_{max}(\text{tungsten}) + I_{max}(\text{Bismuth})} \quad (3)$$

$$W_B = 1 - W_T. \quad (4)$$

were W is the ratio of phase amount, I_{max}(Tungsten) and I_{max}(Bismuth) are the maximal intensity of diffraction peaks of the tungsten bronze phase and bismuth phase, respectively. As shown in the Table 2, the phase constitution deviates from that expected, however, the change trend of phase constitution is right.

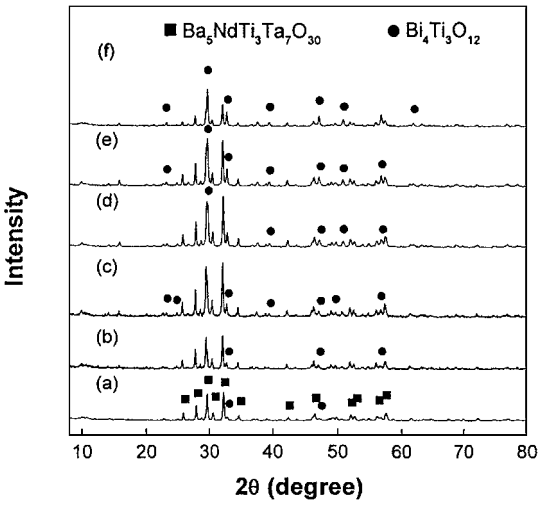

Fig. 6. XRD patterns of $(1-x)(Ba_{0.8}Pb_{0.2})_5NdTi_3Ta_7O_{30}/xBi_4Ti_3O_{12}$ dense ceramics sintered at 1165°C in air for 2 h (a) $x = 0.40$ (sintered at 1180°C), (b) $x = 0.45$, (c) $x = 0.50$, (d) $x = 0.55$, (e) $x = 0.60$, (f) $x = 0.70$.

Table 2. Phase constitution of $(1-x)(Ba_{0.8}Pb_{0.2})_5NdTi_3Ta_7O_{30}/xBi_4Ti_3O_{12}$ dense ceramics.

x	$Ba_5NdTi_3Ta_7O_{30}$ (%)	$Bi_4Ti_3O_{12}$ (%)
0.40	86.2	13.58
0.45	82.6	17.4
0.50	80.0	20.0
0.55	53.5	46.5
0.60	49.2	50.8
0.70	37.5	62.5

The results of SEM observations for the present bi-phase ceramics are shown in Fig. 7. Two phases with different morphologies are apparently observed, and the micrograph varies from columnar to plate-like, as confirmed by XRD analyses.

Figures 8 and 9 illustrate the dielectric properties of the present bi-phase ceramics. The dielectric constant first increases with increasing $Bi_4Ti_3O_{12}$ content, and then decreases when x is more than 0.6. The dielectric loss has the similar tendency. That is, the dielectric loss increases with dielectric constant. But the dielectric loss becomes larger than that of $(1-x)Ba_5NdTi_3Ta_7O_{30}/xBi_4Ti_3O_{12}$ likely due to the volatilization of Pb and Bi or the shorter sintering time. The temperature coefficient of the dielectric constant turns from negative to positive. This change is corresponding to the change of content of the $Bi_4Ti_3O_{12}$ phase. When the content of the $Bi_4Ti_3O_{12}$ phase increases, the temperature coefficient of the dielectric constant becomes more positive, because of the large positive temperature coefficient of the dielectric constant of $Bi_4Ti_3O_{12}$. But it does not agree well with the empirical models for predicting dielectric behavior of

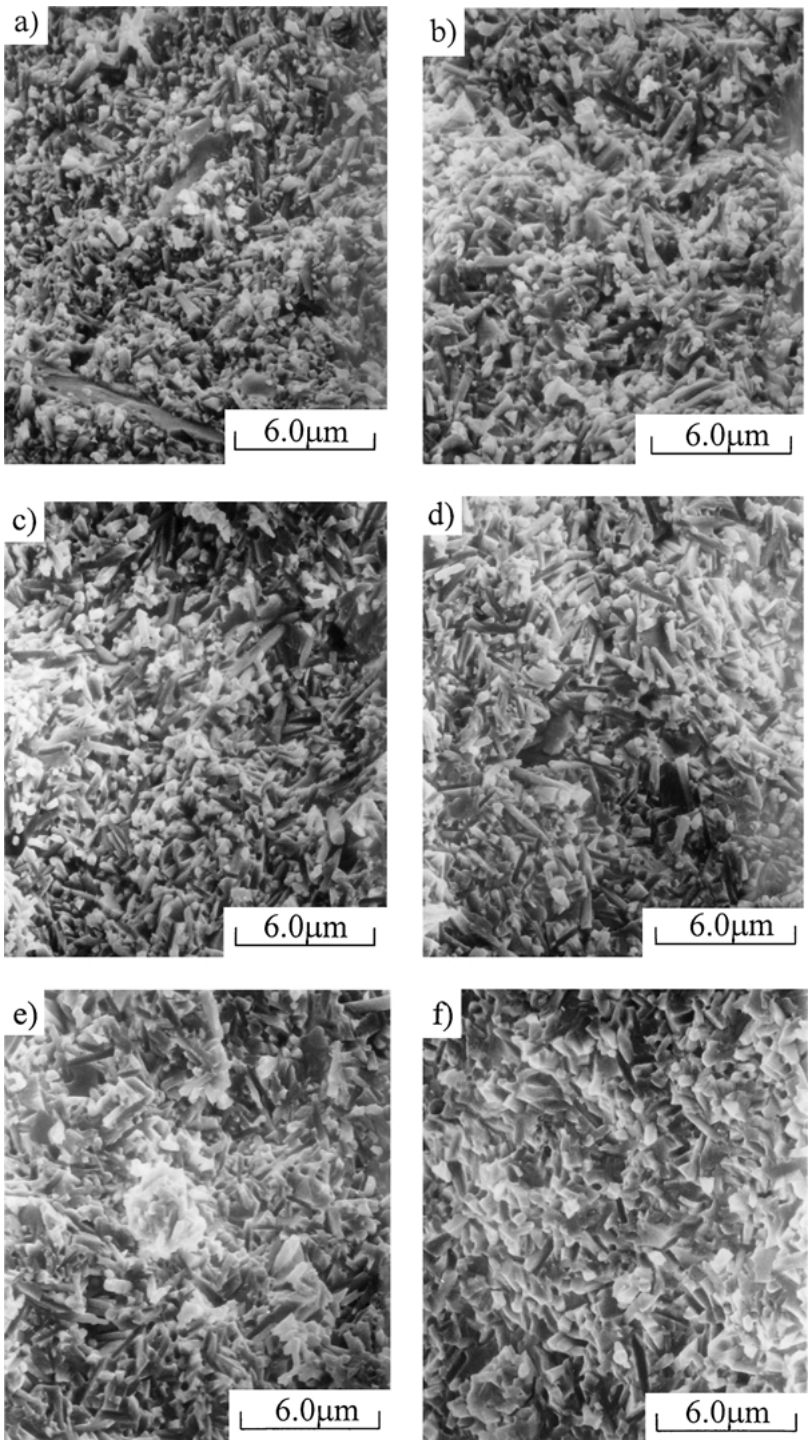

Fig. 7. SEM micrographs of $(1-x)(Ba_{0.8}Pb_{0.2})_5NdTi_3Ta_7O_{30}/xBi_4Ti_3O_{12}$ ceramics sintered at 1165°C in air for 2 h (a) $x = 0.40$ (sintered at 1180°C), (b) $x = 0.45$, (c) $x = 0.50$, (d) $x = 0.55$, (e) $x = 0.60$, (f) $x = 0.70$.

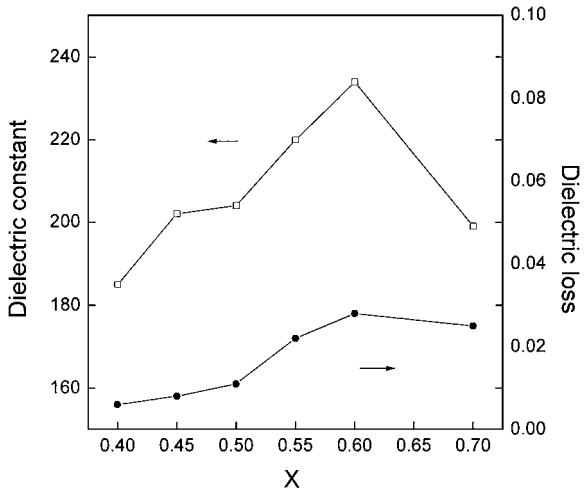

Fig. 8. Dielectric constant and dielectric loss of $(1-x)(Ba_{0.8}Pb_{0.2})_5NdTi_3Ta_7O_{30}/xBi_4Ti_3O_{12}$ ceramics vs composition. Sintering conditions: 1180°C for 2 h for $x = 0.40$ and 1165°C for 2 h for other compositions. Sintered at 1165°C (1180°C for $x = 0.40$) for 2 h.

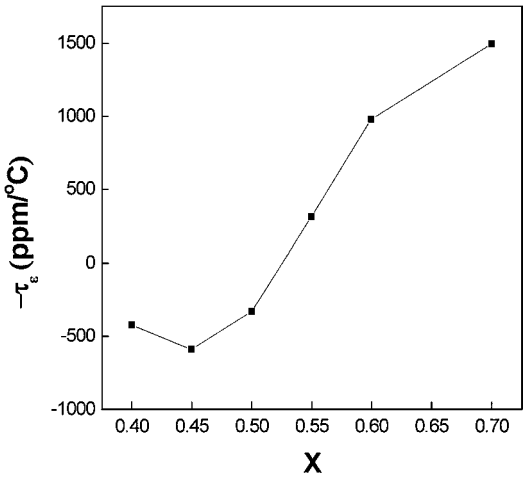

Fig. 9. Temperature coefficient of dielectric constant of $(1-x)(Ba_{0.8}Pb_{0.2})_5NdTi_3Ta_7O_{30}-/xBi_4Ti_3O_{12}$ ceramics vs composition. Sintering conditions: 1180°C for 2 h for $x = 0.40$ and 1165°C for 2 h for other compositions.

mixtures as follows [20]:

$$\ln \varepsilon = V_1 \ln \varepsilon_1 + V_2 \ln \varepsilon_2 \quad (5)$$

$$\tau = V_1 \tau_1 + V_2 \tau_2 \quad (6)$$

where V_1 and V_2 are the volume fractions of the two components, ε_1 and ε_2 are their dielectric constants while ε is the resultant dielectric constant of mixture, and $\tau's$ are the temperature coefficients. When x is between 0.5 and 0.55, the temperature coefficient of the dielectric constant is near zero, and it is negative at $x = 0.5$, but positive at $x = 0.55$, and hence it could be adjusted to zero.

4. Conclusion

The dielectric properties of $Ba_5NdTi_3Ta_7O_{30}$ ceramics were modified through Pb substitution for Ba and the introduction $Bi_4Ti_3O_{12}$ secondary phase. The high dielectric constant ($\varepsilon = 150$) and low dielectric loss ($\tan\delta = 0.0007$) were achieved together with suppressed temperature dependence (τ_ε improved from -2500 ppm/°C to -1279 ppm/°C for $(Ba_{1-x}Pb_x)_5NdTi_3Ta_7O_{30}$ at $x = 0.05$). By introducing $Bi_4Ti_3O_{12}$, temperature-stable dielectric ceramics with high dielectric constant ($\varepsilon > 180$) were obtained when $x = 0.55$ for $(1-x)(Ba_{0.8}Pb_{0.2})_5NdTi_3Ta_7O_{30}/x\,Bi_4Ti_3O_{12}$. However, the dielectric loss associated with Pb substitution for Ba and the introduction of $Bi_4Ti_3O_{12}$ was a problem.

Acknowledgments

The present work was supported by the National Science Foundation for Distinguished Young Scholars under grant No. 50025205 and Special Program for Outstanding Young Scientists of Zhejiang Province under grant No. RC980028.

References

1. M.H. Fremconbe, *Acta Cryst*., **13**, 131 (1960).
2. J.J. Rubin, L.B. Van Uitert, and H.J. Levinstein, *J. Cryst. Growth*, **1**, 315 (1967).
3. R.R. Neurgaonkar, W.F. Hall, J.R. Oliver, W.W. Ho, and W.K. Cory, *Ferroelectrics*, **87**, 167 (1988).
4. A. Bhanumathi, S. Narayana Murty, K. Umakantham, K. Chandra Mouli, G. Padmavathi, K. Tirumala Rao, and V. Syamalamba, *Ferroelectrics*, **102**, 173 (1990).
5. X.M. Chen and J.S. Yang, *J. Euro. Ceram. Soc*., **19**, 139 (1999).
6. X.M. Chen, G.L. Lü, J.S. Yang, and Y.J. Wu, *J. Solid State Chem*., **148**, 438 (1999).
7. J. Wang, X.M. Chen, and J.S. Yang, *J. Mater. Sci. Mater. in Elec*., **10**, 483 (1999).
8. X.M. Chen, X.H. Zheng, and J. Wang, *J. Mater. Res*., **16**(10), 2859 (2001).
9. X.H. Zheng and X.M. Chen, *Jpn. J. Appl. Phys*., **40**, 4114 (2001).
10. J. Wang, X.M. Chen, and J.S. Yang, *J. Res. Soc*., **14**(8), 3375 (1999).
11. L.G. Van Uitert and L. Egerton, *J. Appl. Phys*., **32**, 959 (1961).

12. S.L. Swartz, T.R. Shrout, and T. Takenaka, *Am. Ceram. Soc. Bull*., **76**, 59 (1997).
13. D. Kolar, S. Gaberscek, Z. Stadler, and D. Suvorov, *Ferroelectrics*, **27**, 269 (1980).
14. Y.J. Wu and X.M. Chen, *J. Euro. Ceram. Soc*., **19**, 1123 (1999).
15. X.H. Zheng and X.M. Chen, *J. Electroceramics*, in press.
16. R. Roberts, *Phys. Rev*., **76**, 1215 (1949).
17. R.D. Shannon, *Acta Crys*. A, **32**, 751 (1976).
18. R.D. Shannon, *J. Appl. Phys*., **73**, 348 (1993).
19. S.C. Abrahams, S.K. Kurtz, and P.B. Jamieson, *Phys. Rev*., **172**, 551 (1968).
20. A.E. Paladino, *J. Am. Ceram. Soc*., **54**, 168 (1971).